

## Magneto-optical effect of $\text{La}_{0.7}\text{Ca}_{0.3}\text{MnO}_3$ at low temperature

WAN Fan<sup>1, 2,\*</sup> HAN Jia-Guang<sup>1, 2</sup> ZHU Zhi-Yuan<sup>1</sup>

<sup>1</sup>(Shanghai Institute of Applied Physics, the Chinese Academy of Sciences, Shanghai 201800, China)

<sup>2</sup>(Graduate School of the Chinese Academy of Sciences, Beijing 100049, China)

**Abstract** The magneto-optical Kerr effect of  $\text{La}_{0.7}\text{Ca}_{0.3}\text{MnO}_3$  at low temperature in far-infrared terahertz and mid-infrared region from 0.2 to 1.2 eV is theoretically investigated by means of the Drude model. The complex conductivity and dielectric constants are obtained. The spectra of Kerr rotation with different external magnetic fields  $B$  and temperatures  $T$  are numerically analyzed. A large Kerr rotation in mid-infrared region could be explained as the incoherent hopping motion of polarons.

**Key words** Kerr effect, Ellipticity,  $\text{La}_{0.7}\text{Ca}_{0.3}\text{MnO}_3$

**CLC numbers** O482.55, O513

### 1 Introduction

Since the recent discovery of the colossal magneto resistance (CMR) phenomenon in hole-doped manganite,  $\text{La}_{1-x}\text{Ca}_x\text{MnO}_3$  has been widely studied on account of their unique electronic and magnetic properties, which vary with doping concentrations. For doping concentration  $x$  from 0.2 to 0.5, the materials show a transition from a paramagnetic insulator to a ferromagnetic metal near the Curie temperature  $T_c$  [1, 2]. Such insulator-metal (IM) transition phenomena connecting with the CMR feature has attracted considerable interests for they are helpful to understand the mysterious nature of charge stripes in strongly correlated materials. In order to determine the electrical and magnetic properties of  $\text{La}_{0.7}\text{Ca}_{0.3}\text{MnO}_3$ , various methods have been employed such as Hall effect measurements [3], new muon spin relaxation (USR) and neutron spin echo (NSE) measurements [4], temperature-dependent optical spectroscopy measurements [2], and so on. Among them, optical spectroscopy is a powerful tool for investigating the electronic structure of the manganite [5, 6].

In a previous report [7], Simpson et al. measured the optical properties of these materials at low temperature and got a good theoretical statement to match their experimental results in far-infrared THz and mid-infrared region over the frequency from 0.2 to 1.2 eV. But they did not take the external magnetic field into account. Based on their experiment data, in this paper, we report on a theoretical analysis of the magneto-optical Kerr effect (MOKE) of  $\text{La}_{0.7}\text{Ca}_{0.3}\text{MnO}_3$  at low temperature in the above mentioned frequency region because now the MOKE spectroscopy has become a standard and valuable technique to study various magnetic, optical, and electronic characteristics of materials. MOKE spectroscopy is useful to probe the electronic structure of ferromagnets and is less sensitive to surface effect. Moreover, MOKE is sensitive to the magnetic electrons,  $d$  states in the transition-metal ions, and  $d, f$  states in the rare-earth ions [8]. Hence, the MOKE spectroscopy is applicable to many basic problems of materials that have been studied such as spin-orbit coupling, electron spin polarization, and interband or intraband transition, and so on.

Supported by the Major Project of Knowledge Innovation Project of Chinese Academy of Science (No. KJCX2SW-N02)

\*Corresponding author. Fax: +862159553021. Email: wanfan@sinap.ac.cn

Received date: 2005-07-05

## 2 Theoretical analysis of MOKE

Fig. 1 shows the real and imaginary parts of the diagonal elements of the dielectric function, the Kerr rotation, and ellipticity at 10K, which were calculated by means of the Drude model. As we know, the dielectricity is a function that depends on frequency. In general, the dielectric tensor is symmetric in the absence of an external magnetic field. In this case, it can be treated as a scalar. Under the external magnetic field  $B$ , scalar then changes to tensor. If  $z$ -axis is normal to the sample surface,  $B$  is perpendicular to the sample surface in the Cartesian coordinate. Then the dielectric tensor can be presented as follows [9]:

$$\boldsymbol{\varepsilon} = \begin{pmatrix} \varepsilon_{xx} & \varepsilon_{xy} & 0 \\ \varepsilon_{yx} & \varepsilon_{yy} & 0 \\ 0 & 0 & \varepsilon_{zz} \end{pmatrix}$$

In the Drude model framework, the components of the dielectric tensor in presence of the external magnetic field are as follows [10-12]:

$$\begin{aligned} \varepsilon_{xx} = \varepsilon_{yy} &= \varepsilon_b \left[ 1 - \frac{\omega_p^2 (\omega^2 + i\omega\Gamma)}{(\omega^2 + i\omega\Gamma)^2 - \omega^2 \omega_c^2} \right] \\ \varepsilon_{xy} = -\varepsilon_{yx} &= \frac{i\omega_p^2 \varepsilon_b \omega \omega_c}{(\omega^2 + i\omega\Gamma)^2 - \omega^2 \omega_c^2} \\ \varepsilon_{zz} &= \varepsilon_b \left[ 1 - \frac{\omega_p^2}{\omega^2 + i\omega\Gamma} \right] \end{aligned} \quad (1)$$

where  $\varepsilon_b$  is the background dielectric constant,  $\omega_p = \sqrt{Ne^2 / (\varepsilon_0 \varepsilon_b m^*)}$  is the effective plasma frequency,  $N$  and  $m^*$  are the carrier density and effective mass,  $\Gamma$  is the effective scattering rate, and  $\omega_c = eB / m^*$  is the cyclotron frequency, which can be determined from measurements of the absorption or reflection of circularly polarized electromagnetic wave with frequency  $\omega$ . The off-diagonal part of the dielectric tensor  $\varepsilon_{xy}$ , which arises from interband and intraband transition, is reasonable for the magneto-optical effects. The Kerr rotation  $\theta$  and ellipticity  $\phi$  can be calculated from the formula [10, 11, 13]:

$$\Psi = \theta + i\phi = \varepsilon_{xy} / [\sqrt{\varepsilon_{xx}} (1 - \varepsilon_{xx})]$$

## 3 MOKE of $\text{La}_{0.7}\text{Ca}_{0.3}\text{MnO}_3$

According to the previous experimental data, below the IM transition temperature  $T_{\text{IM}} \sim 230\text{K}$   $\text{La}_{0.7}\text{Ca}_{0.3}\text{MnO}_3$  compound dominates in the ferromagnetic metallic phase. Using the above Drude model, we can calculate the MOKE spectrum of  $\text{La}_{0.7}\text{Ca}_{0.3}\text{MnO}_3$  at low temperature 10K. The parameters of this hole-doped manganite were given by Ref [7]:  $\omega_p = 1.15\text{ eV}$ ,  $\Gamma = 23\text{ meV}$ , and  $\varepsilon_b = 4.9$  [14] (because of the difference between the equations mentioned above and Simpson's, we divided the parameter  $\omega_p$  by  $\sqrt{\varepsilon_b}$ , then  $\omega_p = 514\text{ meV}$ ), so we can get the  $\omega_c$  value of about  $0.02\text{ meV}$ .

Under an external magnetic field of  $B = 0.5\text{ T}$ , the numerical results can be derived when these parameters are put into Eqs. (1). It has been suggested that

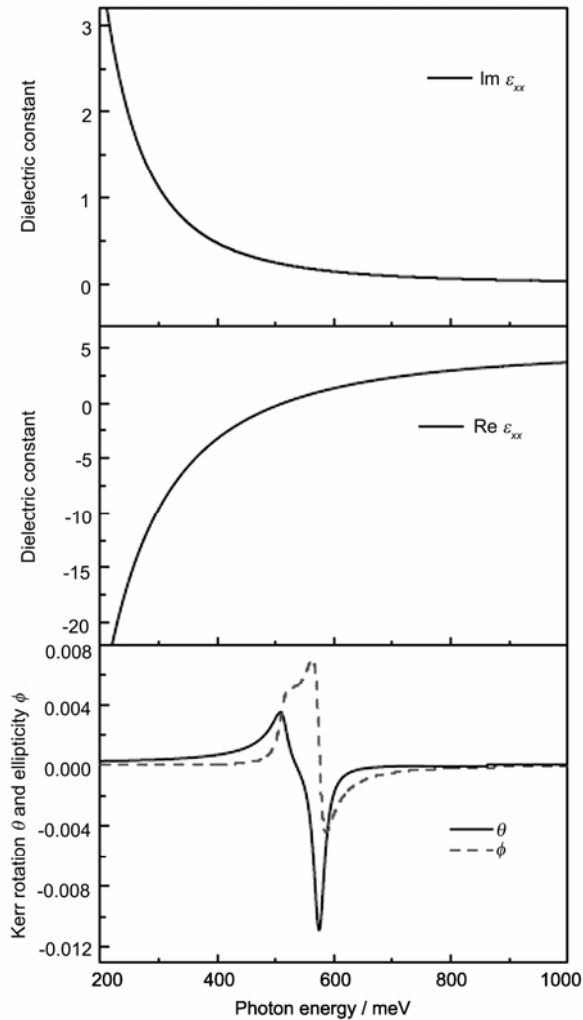


**Fig. 1** The imaginary part and real part of the diagonal element of the dielectric Function  $\varepsilon_{xx}$  at 10K.

(The Kerr rotation  $\theta$  and ellipticity  $\phi$  are also represented.)

around  $\omega_p$ , large resonance-shaped enhancement of Kerr ellipticity will occur while  $\text{Re}(\varepsilon_{xx}) \approx 1.0$  [11, 15]. In a recent study [12], a new viewpoint that the enhancement in the Kerr spectrum occurs at  $\text{Re}(\varepsilon_+, \varepsilon_-) \approx 1.0$  was put forward, while  $\varepsilon_{\pm} = \varepsilon_{xx} \pm \varepsilon_{xy}$ . However in our work, from Fig. 1, the detailed numerical calculation shows that at  $\omega_p$  it is not Kerr ellipticity that reaches its positive maximum, but Kerr rotation, while  $\text{Re}(\varepsilon_{xx})$  is -0.06. When the Kerr rotation gets its minimum value at 574 meV, both  $\text{Re}(\varepsilon_+)$  and  $\text{Re}(\varepsilon_-)$  are equal to 1.0. So is  $\text{Re}(\varepsilon_{xx})$ . On the other hand, from 562 meV to 583 meV the ellipticity reaches its positive and negative values one after another, while  $\text{Re}(\varepsilon_{xx})$ ,  $\text{Re}(\varepsilon_+)$ , and  $\text{Re}(\varepsilon_-)$  are all approximate to 1.0. We think all these happenings may be the reason that at low temperature, the effective damping constant is relatively small compared with the effective plasma frequency. But the true reason is not known clearly yet. As we know, the Kerr effect can manifest many phenomena such as spin-polarization, spin-orbit interaction, plasma edge effect, joint density of states, momentum matrix elements, and so on [16, 17]. In optical frequency domain, the marked enhancement in MOKE spectra originates mainly from the interband and intraband transition. In the low-frequency region, generally, for crystalline, the internal motion, intermolecular modes, and lattice vibrations contribute to low frequency absorption. For  $\text{La}_{0.7}\text{Ca}_{0.3}\text{MnO}_3$ , above  $T_c$ , in the insulating regime it is widely accepted that a small polaron called the ‘‘Holstein polaron’’ plays an important role [2, 18]. Below  $T_c$ ,  $\text{La}_{0.7}\text{Ca}_{0.3}\text{MnO}_3$  is in the ferromagnetic metallic phase, and it was found that  $\text{La}_{0.6}\text{Ca}_{0.4}\text{MnO}_3$  has a large absorption band centered at  $\sim 0.5$  eV. This feature can be attributed to an incoherent hopping motion of polarons from  $\text{Mn}^{3+}$  to  $\text{Mn}^{4+}$  sites in the metallic state and such motion of polarons causes the pronounced enhancement of the MOKE spectra of  $\text{La}_{0.7}\text{Ca}_{0.3}\text{MnO}_3$  [8, 19, 20]. At two sides of  $\omega_p$ , the value of Kerr rotation changes from a positive maximum to a negative maximum. As shown in Fig. 1 when  $\omega = 575$  meV, the Kerr rotation has negative maximum value of  $-0.012^\circ$  while there is a peak of  $0.004^\circ$  at the  $\omega = 507$  meV, which is less than that of normal magnetic materials Fe, Co, and Ni, whose polar rotations are typically in the range of  $0.3^\circ$  to  $0.6^\circ$  for optical frequency [21, 22].

The diagonal and off-diagonal components of optical conductivity tensor  $\sigma_{xx}$  and  $\sigma_{xy}$  have also been calculated by the following equation:

$$\sigma_{\alpha\beta} = -i\omega\varepsilon_0(\varepsilon_{\alpha\beta} - \varepsilon_b\delta_{\alpha\beta}) \quad (2)$$

The subscripts  $\alpha$ ,  $\beta$  can be represented by  $x$  and  $y$ . They are shown in Fig. 2. This is done with  $B=0.5\text{T}$  at 10K temperature. From the figures, it is clear that at the frequency range that has been discussed the real and imaginary parts of  $\sigma_{xx}$  and  $\sigma_{xy}$  are all monotonic. Two parts of  $\sigma_{xx}$  all decrease with the increase in frequency, but variations of two parts of  $\sigma_{xy}$  show opposite tendencies, i.e. the real part decreases with increase in frequency, while the imaginary part increases with frequency increasing. There is another interesting phenomenon, i.e. the frequency  $\omega_p$  is a critical frequency for the real and imaginary parts of conductivity. When frequency  $\omega$  is below  $\omega_p$ , the real and imaginary parts of diagonal and off-diagonal components of optical conductivity tensor change dramatically, exhibiting a strong frequency dependence of them. But when frequency  $\omega$  is above  $\omega_p$ , all curves become smoother. In this range, they present considerable independence of frequency.

The effective scattering  $\Gamma$  has a  $T^2$  temperature dependence [7]. In order to quantify the spectral change with temperature, we have obtained Fig. 3. The values of Kerr rotations below 1.0eV at various temperatures in the ferromagnetic phase are shown. The used optical parameters for numerical calculation of  $\omega_p$  and  $\Gamma$ , given in Table 1, are extracted from the experimental data in Ref. [7]. From Fig. 3, we can see that all enhancements occur at the frequency  $\omega_p$ , whose values at 10K and 70K are almost the same, i.e. their Kerr rotation’s enhancements occur at almost the same place, and so do those at 100K and 130K. In addition, we have found that the Kerr rotation decreases when the temperature increases. Although we have indicated that the apparent enhancement in MOKE spectra of  $\text{La}_{0.7}\text{Ca}_{0.3}\text{MnO}_3$  comes from the incoherent hopping motion of polarons from  $\text{Mn}^{3+}$  to  $\text{Mn}^{4+}$  sites, quantitative information about temperature dependence of this motion is still lacking. From the visible representation of MOKE with different temperatures,

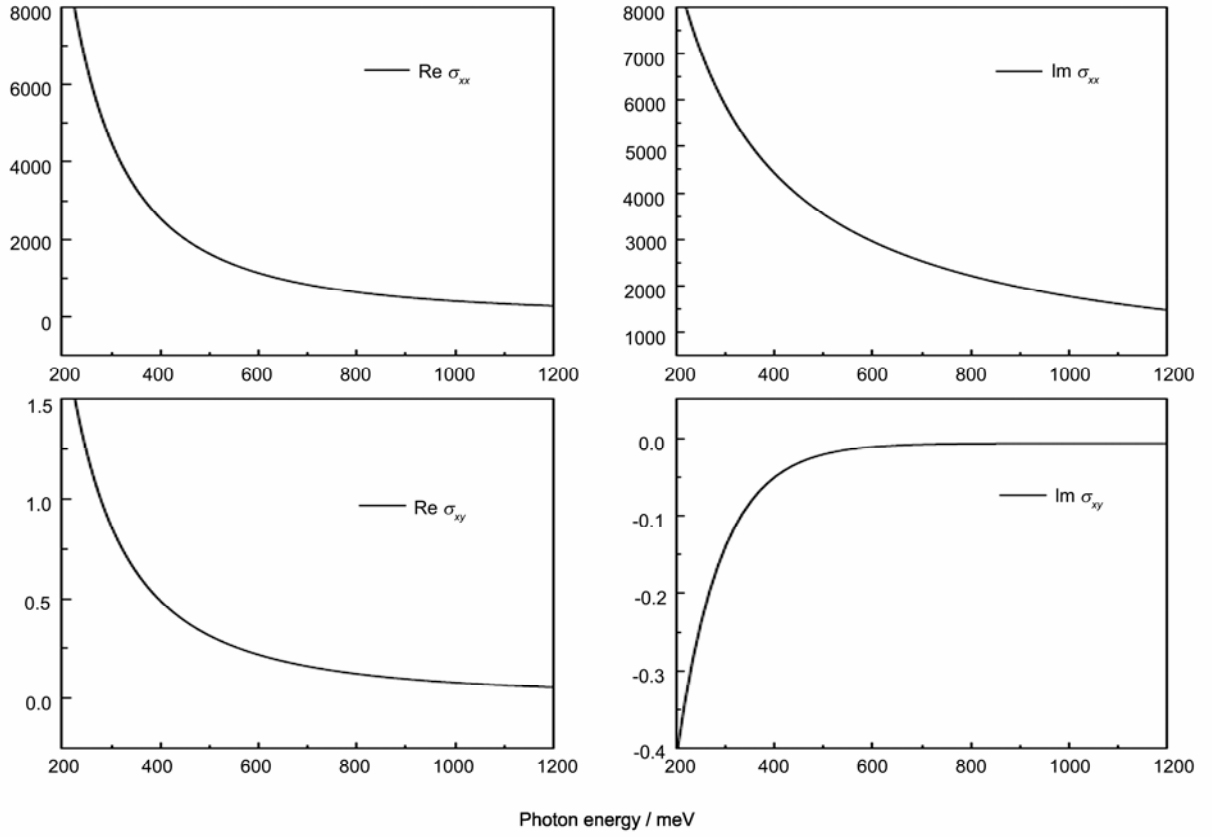


**Fig.2** The imaginary parts and real parts of the diagonal and off-diagonal elements of the conductivity  $\sigma_{xx}$  and  $\sigma_{xy}$ .

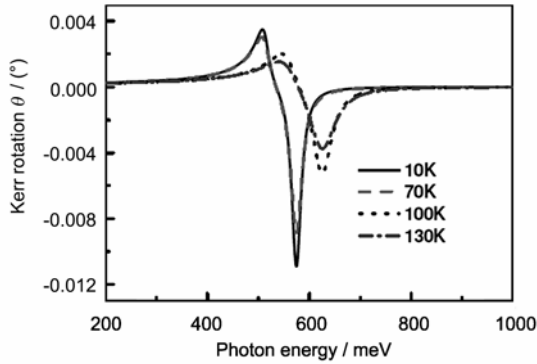


**Fig.3** Calculated Kerr rotations at various temperatures when  $B = 0.5 \text{ T}$ .

**Table 1** Parameters for the MOKE calculation at various temperatures extracted from Ref. [7].

$T / \text{K}$	$\omega_p / \text{meV}$	$\Gamma / \text{meV}$
10K	514	23
70K	523	29
100K	564	46
130K	569	62

we attributed these phenomena to disorder. The effect of magnetic field on a charge inside a magnetized medium is the summation of external magnetic field and magnetization of the medium. When temperature increases, the orientation of magnetization becomes disordered, which results in decrease of the effect on the magnetic field of  $\text{La}_{0.7}\text{Ca}_{0.3}\text{MnO}_3$ . In previous study<sup>[23]</sup>, we can find the data that support our opinion. Although the paramagnetic-to-ferromagnetic transition temperature ( $T_c$ ) is raised in a magnetic field, the phase transformation need not be taken into account, because in the discussed temperature region, the temperature is far below the  $T_c$ .

According to the Drude model, the change of the external magnetic field can affect the Kerr rotation. Fig. 4 shows the Kerr rotation at 10K in different external magnetic fields. From the illustration, we can see that the change of the external magnetic field only affects the values of the Kerr rotation, and the Kerr rotation increases when the external magnetic field

increases. However, all enhancements still occur at the place of  $\omega_p$ . As mentioned above, the MOKE of materials is proportional to the product of the spin-orbit coupling strength and net electron spin polarization. Hence this behavior suggests that the spin-orbit coupling strength and spin polarization are enhanced with increase in the external magnetic field and then result in the increase of MOKE spectra with the increase in the magnetic field.

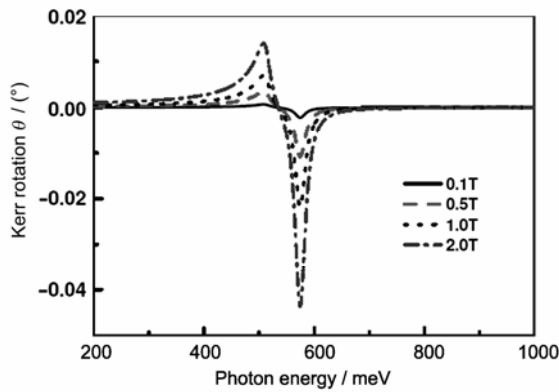


**Fig. 4** Calculated Kerr rotations in various external magnetic fields.

#### 4 Conclusion

In summary, the MOKE of  $\text{La}_{0.7}\text{Ca}_{0.3}\text{MnO}_3$  in low energy region from 0.2 eV to 1.2 eV at low temperature was theoretically calculated with the Drude model. We have shown the enhancement of Kerr effect caused by the motion from  $\text{Mn}^{3+}$  to  $\text{Mn}^{4+}$  sites. The calculated rotation varying between  $0.004^\circ$  and  $-0.012^\circ$  at low temperature was obtained. The Kerr effects of  $\text{La}_{0.7}\text{Ca}_{0.3}\text{MnO}_3$  at different temperatures and in various external magnetic fields were also discussed. The Kerr rotation increases while the temperature decreases because of the disorder. Meanwhile, when the external field increases, the amplitude of Kerr rotation shows a clear increase. We also plotted the real and imaginary parts of diagonal and off-diagonal elements of conductivity as functions of the frequency  $\omega$ . In our paper, we consider the effective scattering rate as a constant independent of frequency  $\omega$  as the Drude model holds, but in fact it also depends on frequency<sup>[7]</sup>. As a macroscopic and experiential model, the Drude model cannot give the microscopic original mechanism. So a more detailed

and comprehensive study is needed in the future.

#### References

- 1 Tokura Y, Tomioka Y. J. Magn. Mater 1999, **200**: 1
- 2 Kim K H, Jung J H, Noh T W. Phys. Rev. Lett. 1998, **81**: 1517
- 3 Chun S H, Salamon M B, Tomioka Y, *et al.* Phys. Rev. B 2000, **61**: R9225
- 4 Heffner R H, Sonier J E, MacLaughlin D E, *et al.* Phys. Rev. Lett. 2000, **85**: 3285
- 5 Okimoto Y, Katsufuji T, Ishikawa T, *et al.* Phys. Rev. B 1997, **55**: 4206
- 6 Takenaka K, Sawaki Y, Sugai S. Phys. Rev. B, 1999, **60**: 13011
- 7 Simpson J R, Drew H D, Smolyaninova V. N, *et al.* Phys. Rev. B, 1999, **60**: R16263
- 8 Yamaguchi S, Okimoto Y, Ishibashi K, *et al.* Phys. Rev. B, 1998, **58**: 6862
- 9 Ino Y, Shimano R, Svirko Y, *et al.* Phys. Rev. B, 2004, **70**: 155101
- 10 Shimano R, Ino Y, Svirko Y, *et al.* Appl. Phys. Lett. 2002, **81**: 199
- 11 Feil H, Hass C. Phys. Rev. Lett. 1987, **58**: 65
- 12 De A, Puri A. J. Appl. Phys. 2003, **93**: 1120
- 13 Argyres P N. Phys. Rev. 1955, **97**: 334.
- 14 Kim K H, Jung J H, Noh T W, *et al.* Phys. Rev. Lett. 1998, **81**: 1517
- 15 Han Jianguang, Zhu Zhiyuan, Liao Yi *et al.* Phys. Lett. A. 2003, **315**: 395
- 16 Ghosh D B, De M, De S K. Phys. Rev. B 67, (2003) 035118
- 17 Han Jianguang, Zhu Zhiyuan, Liao Yi, *et al.* Carbon 2004, **42**: 1793
- 18 Muhlstroh M, Reik H G. Phys. Rev. 1957, **162**: 703
- 19 Kim K H, Lee S, Noh T W, *et al.* Phys. Rev. Lett. 2002, **88**: 167204
- 20 Quijada M, Cerne J, Simpson J R, *et al.* Phys. Rev. B 1998, **58**: 16093
- 21 Kraft T, Oppeneer P M, Antonov V N, *et al.* J. Phys. Rev. B 1995, **52**, 3561
- 22 Oppeneer P M, Maurer T, Sticht J, *et al.* J. Phys. Rev. B 1995, **45**: 10924
- 23 Schiffer P, Ramirez A P, Bao W, *et al.* Phys. Rev. Lett. 1995, **75**: 3336